Redox chemistry over CeO_2-based catalysts: SO_2 reduction by CO or CH_4

Tianli Zhu, Ljiljana Kundakovic, Andreas Dreher[1], Maria Flytzani-Stephanopoulos[*]

Department of Chemical Engineering, Tufts University, Medford, MA 02155, USA

Abstract

The catalytic reduction of SO_2 to elemental sulfur by CO and CH_4 over Cu-modified ceria catalysts is studied in this work. Doped and undoped ceria are active catalysts for the SO_2 reduction by CO or CH_4 in the temperature range 450–750°C. When CO is used as the reductant, the reaction follows the redox mechanism, and formation of surface defects (oxygen vacancies) and ceria reducibility are important for catalyst activity. SO_2 strongly adsorbs on the catalyst surface forming sulfates. Partial reduction of sulfate by CO is necessary for the reaction to light off and proceed at low temperatures. Addition of copper improves the low-temperature catalyst activity by increasing the reducibility of ceria and providing sites for CO adsorption. On the other hand, methane activation is limited by the thermal stability of surface sulfates. The activation of methane may involve surface oxygen species and partially reduced metal oxide sites at high temperature. Two independent reactions are proposed and used to explain the catalytic performance of ceria-based oxides in CH_4+SO_2 gas mixtures. One reaction leads to elemental sulfur and complete oxidation (CO_2+H_2O) products, while the second produces H_2S and $CO+H_2O$ under fuel-rich conditions. The addition of copper suppresses the latter, thus increasing the catalyst selectivity to elemental sulfur. The catalyst activity/selectivity studies were complemented by SO_2 uptake experiments in a TGA and reduction studies of the as-prepared and pre-sulfated catalysts in CO and methane, both isothermally and in the TPR mode. © 1999 Elsevier Science B.V. All rights reserved.

Keywords: Cerium oxide catalysts; Redox mechanism; Sulfur recovery; Sulfur dioxide reduction; Carbon monoxide; Methane; Copper and cerium oxide; Elemental sulfur

1. Introduction

Sulfur dioxide, an ubiquitous component of fuel combustion exhausts and one of the first air pollutants to be regulated in the US and abroad, continues to be challenging to control in a cost-effective and environmentally sound manner. At the present time, sulfur dioxide removal via scrubbing is the method of choice. Highly efficient SO_2 scrubber systems are now commercially available and their cost is gradually declining. However, the large amount of solid waste generated from these systems is a potential environmental problem and waste disposal entails continually increasing landfill costs.

More than 170 wet scrubber systems applied to 72 000 MW of US coal-fired, utility boilers are currently in operation [1]. A small fraction (of the order 1

*Corresponding author. E-mail: mstephanopoulos@infonet.tufts.edu

[1]Present address: Institute of Energy Engineering, Technical University of Berlin, Germany.

percent [2]) of these systems produces a usable byproduct (gypsum), while the remainder generate approximately 20 million tons per annum of disposable flue gas desulfurization (FGD) byproduct, which are transported and disposed of in landfills [3]. The use of regenerable sorbent technologies has the potential to reduce or eliminate this solid waste production, transportation and disposal.

All regenerable FGD systems produce an off-gas stream from the regenerator that must be processed further in order to obtain a saleable byproduct, such as elemental sulfur, sulfuric acid or liquid SO_2. This off-gas stream is only a fraction of the flue gas volume, and contains no oxygen. Recovery of elemental sulfur from this stream in a single-stage catalytic converter, avoiding a multi-stage Claus plant, would decrease the cost and accelerate the commercialization of many regenerable FGD processes. Even when there is no market for the sulfur, elemental sulfur constitutes only one-third of the volume of the equivalent $CaSO_4$ byproduct, and is completely innocuous. Therefore, no secondary pollution issues ensue from this approach.

The use of catalysts for the direct conversion of SO_2 to elemental sulfur has been explored many times in the past. Both a high catalyst activity and a high selectivity to sulfur are required to avoid complex schemes or multi-stage processes, such as in Claus plants. A main barrier to further development of various active catalysts identified in the literature has been the lack of suitable selectivity.

Various reductants have been used for SO_2 reduction, including CO, H_2, CH_4 and carbon. The overall reactions between SO_2 and CO or CH_4 to elemental sulfur product may be written as:

$$SO_2 + 2CO \rightarrow [S] + 2CO_2 \qquad (1)$$

$$2SO_2 + CH_4 \rightarrow CO_2 + 2H_2O + 2[S] \qquad (2)$$

where [S] represents the various elemental sulfur forms (S_2, S_6, S_8). Under fuel-rich conditions, COS is the primary byproduct for reaction 1, while a thermodynamic analysis shows that the product mixture for reaction 2 may also contain H_2S, COS, CS_2, CO and H_2. Most previous studies of reduction of SO_2 to elemental sulfur examined carbon monoxide as the reductant [4–12]. A variety of catalyst materials have been studied, including transition metals and mixed

oxides. The perovskite-type mixed oxides have received a lot of attention. A class of ABO_3-type mixed oxides consisting of alkaline earth, rare earth, and transition metal elements were disclosed in a patent by Whelan [4]. Happel and coworkers [5,6] proposed a redox reaction mechanism involving surface oxygen/oxygen vacancy participation for La–Ti–O perovskite oxide catalysts. The SO_2 reaction with CO over $Sr_xLa_{1-x}CoO_3$ perovskite catalysts was also discussed within the redox framework by Hibbert and Campbell [7,8]. Perovskite oxides, such as $LaCoO_3$, have both excellent electronic conductivity and oxygen ion mobility [9]. These studies have suggested that oxygen vacancy or mobility may be an important catalyst property for SO_2 reduction by CO. However, perovskite oxides are not stable under the reaction conditions and decompose into metal sulfide and oxysulfide. The COS reaction intermediate mechanism was proposed for this type of catalysts [10], that is, CO reacts with SO_2 over metal sulfides to form COS and then, COS reduces SO_2 to elemental sulfur.

A single-stage catalytic process for the conversion of SO_2 to sulfur is under development at the Lawrence Berkeley Laboratory using mixed metal oxide catalysts on alumina support [11]. Sulfur yields as high as 98% have been reported at 500°C with dry or wet syngas as the reductant at atmospheric pressure and low space velocity (2100 h^{-1}). Another process under development is the direct sulfur recovery process (DSRP) at the Research Triangle Institute [12]. This reports high sulfur yields at 627°C at relatively low space velocities (3750 h^{-1}) and high pressure (21.4 atm). Recently, we have reported that fluorite-type oxides, such as cerium oxide and stabilized zirconium oxide, are highly active and selective catalysts for the SO_2 reduction by CO [13–16]. Thus, more than 97% sulfur yield and complete conversion of SO_2 were obtained over a modified cerium oxide catalyst at 470°C, at SV=45 000 h^{-1} and atmospheric pressure [15].

SO_2 reduction by methane is more difficult to achieve due to the refractory nature of methane. The catalysts considered for this reaction include bauxite [17], alumina [18], transition metal sulfides [19,20], and alumina-supported catalysts [21–24]. Several recent studies have focused on supported molybdenum sulfide catalysts using concentrated SO_2 mixtures [20,22,23]. In all cases a molybdenum

content higher than 15 wt% was necessary for a high catalyst activity irrespective of the type of support. This was attributed to the need for the formation of MoS_2 crystal cluster on the support surface [22]. Cobalt oxide was recently reported as an active catalyst over alumina [24], at higher temperatures 700–820°C. CoS_2, identified by XRD in the used sample, was thought to be the active phase for the reaction between SO_2 and CH_4. That the mechanism involves formation of [S] via intermediate H_2S [22] seems to be a reasonable conclusion for these catalysts, since MoS_2 and CoS_2 are active catalysts for H_2S decomposition [25–27], while alumina itself is active for the Claus reaction. Because sulfur is a secondary product over these catalysts (produced from H_2S intermediate), the sulfur yield is maximized at very low space velocity. The optimized ratio of SO_2/CH_4 used by various authors [20,21,28] was typically higher than the stoichiometric ratio of 2:1 (reaction 2) to increase the catalyst activity at low temperature.

A different reaction mechanism is displayed over cerium oxide-based catalysts. We have recently reported that the SO_2 reduction by CO on ceria-based catalysts follows the redox mechanism [13–16]. The redox reaction framework consists of cyclic reduction of the catalyst surface by CO and oxidation of the catalyst surface by SO_2. Reduction by CO produces oxygen vacancies that are taken up by SO_2, which is thereby reduced to elemental sulfur. Thus, sulfur is a primary product and very high space velocity can be used without affecting the sulfur yield. The formation of surface oxygen vacancies by CO reduction is an important step in catalyst activation [15,16]. The created surface oxygen vacancies can also be capped by other oxidizing agents, such as carbon dioxide and water. The catalytic activity and resistance to water vapor of cerium oxides can be significantly enhanced by addition of small amounts of a transition metal, such as copper [15,16].

High reducibility and oxygen mobility as well as high oxygen vacancy concentration are the reasons for the high catalytic activity of ceria in redox reactions [15,29]. The bulk and surface properties of CeO_2 can be modified by doping [30]. Doping can improve the sintering properties of ceria, by stabilizing the ceria surface area and crystal size. Doping with divalent and trivalent dopants leads to the formation of oxygen vacancies, and modification of oxygen mobility and

ionic conductivity [31,32]. The reduction properties and oxygen storage capacity of ceria are also reported to change by doping. Ce–Zr–O solid solutions were extensively studied recently because of their unusual reduction behavior and high oxygen storage capacity [33–35]. These properties were attributed to the formation of a defective fluorite oxide-type structure by introduction of the smaller Zr^{4+} ion into the cerium oxide structure, which leads to higher oxygen mobility [36].

In this paper, we report on the catalytic activity/selectivity of ceria-based catalysts for the reduction of SO_2 by CO or CH_4 at the relatively high space velocity of 20 000–80 000 h^{-1} (STP). The performance of catalysts was addressed in terms of dopant and metal effect. The catalytic properties of ceria-based oxides for these reactions are discussed within the redox framework.

2. Experimental

2.1. Catalyst preparation and characterization

Bulk catalysts (ceria, (La/Zr) doped ceria as well as copper-containing cerium (La/Zr) oxides) were prepared by the urea gelation/coprecipitation method using metal nitrates and urea [37]. This method provides well-dispersed and homogeneous mixed metal oxides. The preparation procedure consists of the following steps:

1. mixing nitrate salts of metals with urea and heating the solution to 100°C under continuous stirring;
2. after coprecipitation, boiling the resulting gels vigorously for 8 h;
3. filtering and washing the precipitate twice with hot deionized water;
4. drying the precipitate overnight in a vacuum oven at 110°C;
5. crushing the dried lumps into powder and calcining in static air for 3 h at 650°C reached at a heating rate of 2°C/min.

The samples used for the SO_2 and CH_4 reaction were further heated at 720°C for 3 h. The typical packing density of the thus prepared catalysts was around 2 g/cm^3 and their surface area was 65–70 m^2/g (undoped

ceria similarly prepared had a surface area of 45 m^2/g). The dopant level in all materials is expressed in atomic metal percent, e.g. for lanthanum, as La/(La+Ce)×100%.

The total catalyst surface area was measured by single-point N$_2$ adsorption/desorption on a Micromeritics Pulse ChemiSorb 2705 instrument. For bulk composition analysis, the catalyst powder was dissolved in a 70% HNO$_3$ acid solution (ACS reagent) and diluted with de-ionized water. The resulting solution was analyzed by inductively coupled plasma (ICP) atomic emission spectrometry (Perkin Elmer Plasma 40). X-ray powder diffraction (XRD) analysis of the catalyst samples was performed on a Rigaku 300 X-ray Diffractometer with rotating anode generators and monochromatic detector. Copper K$_\alpha$ radiation was used with a power setting at 60 kV and 300 mA. For crystal phase identification, the typical operation parameters were: divergence slit of 1°, scattering slit 1°, receiving slit 0.3°, and a scanning rate of 2°/min with 0.02° data interval. The crystal size of ceria was calculated from the XRD peak broadening using the Scherrer equation. The surface composition of the catalysts was analyzed by X-ray photoelectron spectroscopy (XPS) on a Perkin Elmer 5100C system. All measurements were carried out at room temperature and without any sample pre-treatment. A Mg K$_\alpha$ X-ray source was primarily used in this work. The X-ray generator power was typically set at 15 kV and 20 mA.

2.2. Apparatus and procedure

2.2.1. Activity experiments

Catalyst activity tests were conducted in a laboratory-scale, packed-bed flow reactor made of quartz (i.d.=1.0 cm) with a porous quartz frit supporting the catalyst. All catalysts were in powder form (<150 µm). The reactor was heated inside a Lindberg electric furnace. The temperature was measured by a quartz tube-sheathed K-type thermocouple placed at the top of the packed bed, and was controlled by a Wizard temperature controller. The reacting gases, all certified calibration gas mixtures with helium (Middlesex), were measured by mass flow controllers and mixed prior to the reactor inlet. The mol percentage of SO$_2$ in the feed gas was typically unity. The experiments were carried out under nearly atmospheric

pressure. A cold trap connected at the outlet of the reactor was used to separate and collect the elemental sulfur and water from the product gas stream. The reactants and products were analyzed by an on-line HP5880A gas chromatograph (GC) equipped with a thermal conductivity detector (TCD). A 1/8 in. o.d.×6 in. long Teflon column packed with Poropak QS was employed to separate CH$_4$, CO, CO$_2$, COS, CS$_2$, H$_2$S and SO$_2$, while a 1/4 in. o.d.×6 in. long glass Chromosil 310 column was used to separate CO, CO$_2$, COS, CS$_2$, H$_2$S and SO$_2$ in the SO$_2$+CO reaction tests.

The following notation is used throughout the paper:

$$R = [CO]_{in} \text{ or } [CH_4]_{in}/[SO_2]_{in}$$

$$X - SO_2 = ([SO_2]_{in} - [SO_2]_{out})/[SO_2]_{in}$$

$$Y - H_2S = [H_2S]_{out}/[SO_2]_{in}$$

$$Y - [S] = [Sulfur]_{out}/[SO_2]_{in}$$

$$S = Y - [S]/X - SO_2$$

where [CO]$_{in}$, [CH$_4$]$_{in}$ and [SO$_2$]$_{in}$ are mol percentages of CO, CH$_4$ or SO$_2$ in the feed gas, and [Sulfur]$_{out}$, [SO$_2$]$_{out}$ and [H$_2$S]$_{out}$ are mol percentages of elemental sulfur, SO$_2$ and H$_2$S in the effluent gas, respectively. Typically, [Sulfur]$_{out}$ was determined by subtracting the mol percentages of H$_2$S and COS in the effluent gas from the difference of [SO$_2$]$_{in}$–[SO$_2$]$_{out}$. Occasionally, a gravimetric measurement was used to determine the amount of sulfur collected in the trap. The sulfur balance was typically better than 90%. X-SO$_2$, Y-H$_2$S, Y-[S] and S, denote the conversion of SO$_2$, H$_2$S yield, sulfur yield, and selectivity to elemental sulfur, respectively.

2.2.2. Temperature-programmed reduction (TPR) experiments

Temperature-programmed reduction (TPR) of the as-prepared catalysts in fine powder form (<150 µm) was carried out in a Cahn TG 121 thermogravimetric analyzer (TGA). The catalysts were preheated to 500°C in a 5%O$_2$/He mixture (50 cm^3/min (STP)) for 30 min. After cooling down to room temperature in the O$_2$/He mixture followed by flushing in He, the samples were heated in a 5%CH$_4$/He or 5%H$_2$/He or 2%CO/He gas mixture (150 cm^3/min (STP)) at a heating rate of 10°C/min to 750°C, while monitoring

the catalyst weight change in the TGA. TPR of pre-sulfated catalysts was conducted in the packed-bed reactor with on-line mass spectrometry. For this study, 150 mg of catalyst was loaded into the quartz tube reactor. The catalyst was preheated to 400°C in He and stabilized for 30 min before the introduction of 1%SO_2/He (50 cm³/min (STP)). After the catalyst was exposed to the SO_2 stream for 30 min, the reactor was cooled down to room temperature in the same stream. The catalyst was then flushed with He and heated in a 2%CH_4/He or 2%CO/He gas mixture at a heating rate of 10°C/min to 750°C. The flow rate of the reducing gas was typically 50 cm³/min. The effluent gas composition and intensity were followed by mass spectrometry (MS) using a quadrupole residual gas analyzer (MKS-model RS-1). The experimental operation variables in TPR were such as to keep the parameter $P = \beta S_0 / V C_0$ proposed by Malet and Caballero [38] as low as possible, and in any case lower than 20 K. Here, S_0 is the initial amount of reducible species, V the total flow rate, C_0 the initial reductant concentration in the feed gas and β is the heating rate.

2.2.3. Isothermal SO_2 uptake and reduction experiments in the TGA

Tests to measure the SO_2 uptake capacity of fresh catalysts and the reducibility of pre-sulfated catalysts were conducted in the TGA apparatus. A sample of a few mg was loaded into a quartz pan. The temperature was raised to a given value in pure He (600 cm³/min (STP)) and after the system was stabilized, 1% SO_2/He gas mixture (600 cm³/min (STP)) was introduced. After exposing the catalyst to the SO_2 stream for about 30 min, a mixture of 4% CH_4/He (600 cm³/min (STP)) was introduced and isothermal reduction began. Data were acquired every 10 s during these experiments. The SO_2 uptake curves are plotted as the relative weight change $\Delta W/W_0/SA \times 100\%$ versus temperature, in which ΔW represents the weight change (g) due to the uptake of SO_2; W_0 and SA are the initial weight (g) and total surface area (m²) of the sample, respectively. The isothermal reduction curves are plotted as (1-conversion)×100% versus time, in which conversion is defined as ($\Delta W/W_S$), where ΔW is the sample weight drop (g) due to reduction, and W_S is the sample weight change (g) at the end of sulfation, i.e., the amount of SO_2 uptake.
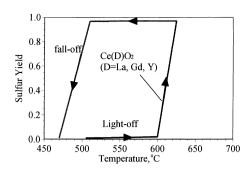

Fig. 1. Sulfur yields over fluorite-type doped cerium oxides for the SO_2 reduction by CO (1%SO_2–2%CO–He, 0.03 g s/cm³ (STP)), [15].

3. Results and discussion

3.1. SO_2 reduction by CO

A typical SO_2 conversion/sulfur yield profile for the stoichiometric SO_2 reduction by CO over doped cerium oxide, Ce(D)O_2, is shown in Fig. 1. Only the sulfur yield is presented in Fig. 1 since COS is a negligible byproduct under these conditions, so that the sulfur yield represents the SO_2 conversion. When the reaction is started with a fresh catalyst without any pre-treatment and the temperature is slowly raised, reaction light-off occurs at about 600°C over the La-doped ceria catalyst. After activation, the reaction temperature could be lowered to 500°C. This hysteresis behavior was observed with all fresh catalysts. However, catalysts pre-treated by reduction in CO (10%CO/He, 2 h at 600°C) prior to the activity measurement did not show any hysteresis. These observations are understood by the proposed redox mechanism. Surface reduction by CO is still a key step to initiate the reaction. However, under reaction conditions, CO and SO_2 would compete for surface oxygen. Reaction of CO with the surface capping oxygen produces CO_2 and an oxygen vacancy, while reaction of SO_2 with the surface oxygen forms sulfate [16]. Under reaction conditions, the rate of the surface oxygen reduction by CO has to be greater than the rate of surface sulfation by SO_2. After the surface oxygen and sulfate are removed, the redox reaction can operate at lower temperature.

Oxygen vacancy formation and cerium oxide reducibility are important in the catalytic reduction of SO_2 by CO. The ceria reduction properties can be modified
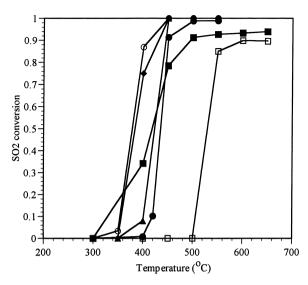
Fig. 2. Light-off behavior of several cerium oxide-based catalysts (0.09 g s/cm^3 (STP); 1%SO$_2$–2%CO; 1%SO$_2$–1.86%CO for CeO$_2$-urea, 1%SO$_2$–1.8%CO for CeO$_2$-acetate), (■) CeO$_2$-urea, (□) CeO$_2$-acetate, (▲) Ce(10%La)O$_2$, (◆) Ce(10%Zr)O$_2$ (●) Ce(50%Zr)O$_2$, (○) 5%Cu–Ce(50%Zr)O$_2$.

by doping [15,30]. Doping with trivalent dopants also introduces extrinsic oxygen vacancies. In addition, non-stoichiometric ceria was identified in nanocrystalline materials synthesized by controlled gas condensation [29]. Here, we discuss the oxygen vacancy formation by decreasing the crystal size of ceria when La and Zr are used as dopants, and its effect on the catalyst activity.

The light-off behavior of various activated (pre-reduced) undoped and doped cerium oxide catalysts for the SO$_2$ reduction by CO is shown in Fig. 2. The materials were activated by reduction in 10% CO for 2h at 600°C prior to testing. The CO/SO$_2$ ratio was 2 for all experiments except for the undoped ceria (the CO/SO$_2$ ratio was 1.86 for the CeO$_2$-urea and 1.80 for the CeO$_2$-acetate). Thus, for the undoped cerias the conversion of SO$_2$ is lower than 100% due to the lower CO/SO$_2$ ratio used. The surface area and crystal size of ceria as determined by XRD analysis are shown in Table 1. All materials shown had the cubic (fcc) crystal structure. Both undoped and doped cerium oxides are active catalysts for the catalytic reduction of SO$_2$ by CO, with a temperature for 80% SO$_2$ conversion of ∼420°C at 70 000 h^{-1} (STP). A strong effect of ceria crystallinity on the redox activity is evident. Nanocrystalline undoped cerium oxide prepared by the urea coprecipitation with a 9.4 nm crystal size shows 50% SO$_2$ conversion at 420°C. For the ceria prepared from thermal decomposition of the acetate with the larger crystal size of 20 nm, the light-off temperature for 50% conversion shifts to higher temperature (520°C). Both Zr and La dopants decrease the crystal size of ceria below 8 nm and are more active than undoped ceria (Fig. 2). On Ce(10%La)O$_x$, 50% conversion of SO$_2$ is measured at 400°C, while Ce(10%Zr)O$_x$ is the most active among the catalysts studied giving 50% conversion of SO$_2$ at 350°C. Moreover, both La and Zr dopants increase the reducibility of ceria. A measure of the reduction extent is given by the value of x in CeO$_x$ in H$_2$-TPR as shown in Table 2. The Ce(10%La)O$_x$ catalyst is reduced at lower temperature than the undoped ceria (value of x is 1.96 at 300°C for Ce(10%La)O$_x$ catalyst compared to 1.99 for CeO$_2$). At the same dopant level (10%), Zr-doped ceria is

Table 1
BET surface area and crystal size of pure and doped CeO$_2$

Catalyst[a] (calcination temperature)	BET surface area (m^2/g)	Crystal size (nm)
CeO$_2$ (650°C)	70.2	9.4
CeO$_2$ (750°C)[a]	18	20.0
Ce(10%Zr)O$_2$ (650°C)	101	6.8
Ce(50%Zr)O$_2$ (650°C)	119.9	4.1
Ce(4.5%La)O$_2$ (650°C)	69.7	8.1
Ce(10%La)O$_2$ (650°C)	91.7	7.2
5%CuCe(4.5%La)O$_2$ (650°C)	92.1	12.1
5%CuCe(50%Zr)O$_2$ (650°C)	87.6	n.d.

[a]Prepared by the urea precipitation/gelation method [37].
[b]From cerium acetate decomposition.

Table 2
H_2-TPR of ceria catalysts[a]

Catalyst (calcination temperature)	Reduction temperature (°C)							
	170	200	300	400	450	500	600	850
CeO_2 (650°C)	2.00	2.00	1.99	1.98	1.97	1.96	1.93	1.75
Ce(10%Zr)O_2 (650°C)	1.96	1.95	1.92	1.90	1.88	1.85	1.73	1.60
Ce(50%Zr)O_2 (650°C)	1.97	1.95	1.91	1.86	1.81	1.72	1.53	1.38
Ce(4.5%La)O_2 (650°C)	2.00	2.00	1.99	1.98	1.98	1.96	1.90	1.75
Ce(10%La)O_2 (650°C)	1.97	1.96	1.96	1.94	1.93	1.91	1.84	1.73
5%CuCe(50%Zr)O_2 (650°C)[b]	1.87	1.84	1.76	1.69	1.64	1.59	1.52	1.38
5%CuCe(4.5%La)O_2 (650°C)[b]	1.96	1.93	1.91	1.88	1.86	1.84	1.78	1.66

[a]Reduction extent expressed as x in CeO_x. TPR conditions: 5%H_2/He, 500 cm³/min (STP), 10°C/min in the TGA.
[b]Reduction extent expressed as x in CeO_x assuming that all CuO was reduced to copper metal.

more reducible than the La-doped ceria, as is evident from the reduction extents given in Table 2.

Nanocrystalline ceria is highly defective and its properties are different than those of well-crystallized materials. Nanocrystalline ceria has lower grain boundary resistance, higher electronic conductivity and lower heat of reduction than coarse-grained materials [39]. In the SO_2 reduction by CO, the hypothesized redox reaction mechanism involves formation of surface oxygen vacancies. Both La and Zr dopants decrease the crystal size of ceria (Table 1) to about 7 nm after the 650°C heat treatment and increase its reducibility (Table 2). However, the activity of Zr-doped ceria is higher than that of La-doped ceria, although La as a dopant also leads to formation of extrinsic oxygen vacancies. Activity tests have suggested that the higher catalytic activity derives from the enhanced reducibility of the material, as shown in Table 2. The data in Fig. 2 support these arguments except for Ce(50%Zr)O_x. Although the crystal size of Ce(50%Zr)O_x (4.1 nm) is lower than that of Ce(10%Zr)O_x (6.8 nm), its activity is lower (50% conversion of SO_2 at 420°C, Fig. 2). This somewhat unusual behavior may be the result of the lower content of ceria in these catalysts. For example, the amount of oxygen removed per total metals present (atoms O/total metal atoms) at 600°C is 0.243 for Ce(10%Zr)O_2 and 0.235 for Ce(50%Zr)O_2. The overall reducibility of Ce(10%Zr)O_2 is thus, slightly higher than that of Ce(50%Zr)O_2. Redox reactions on ceria require Ce–O–Ce redox couples for electron transfer, so that a lower concentration of these couples would lead to lower activity. Partial tetragonalization of the Ce(50%Zr)O_x solid solution may be another

reason for the observed lower activity. The formation of tetragonal phase in Ce(50%Zr)O_x solid solutions has been reported in the literatures [34,40]; however, this phase was not detected in this work.

Addition of a transition metal, such as copper, significantly improves the cerium oxide catalyst activity and its resistance to water and carbon dioxide poisoning. As shown in Fig. 2 for 5%Cu-Ce(50%-Zr)O_x, the temperature for 50% conversion of SO_2 is about 350°C for the pre-reduced (activated) catalyst. The same light-off behavior was found for another copper-containing La-doped ceria catalyst, 5%Cu–Ce(4.5%La)O_x (data not shown).

It is known that addition of noble metals (Pt, Pd, Rh) increases the reactivity of low-temperature oxygen species formed on ceria [41–48]. As a result, the reducibility of ceria at low temperatures is enhanced [49,50]. Recent reports have shown that the oxidation activity of ceria can be largely enhanced not only by the platinum metals but also by transition metals in general [15,51–56]. Similarly to noble metals, copper enhances the reducibility of ceria at low temperatures as it is illustrated in Fig. 3 and Table 2. For example, the reduction extent, x, at 500°C is 1.84 for the 5%Cu-Ce(4.5%La)O_x and 1.96 for Ce(4.5%La)O_x as shown in Table 2. The low-temperature reducibility of ceria resulting from the presence of copper benefits the catalyst activity for oxidation reactions. Extensive characterization analyses of fresh Cu-Ce(La)O_x catalysts by XPS, XRD and STEM/EDX were recently reported [15,16,53,54]. No CuO was detected in the as prepared materials after air calcination at 650°C at copper contents lower than 15 at%. Copper was distributed in the cerium oxide matrix in the form of
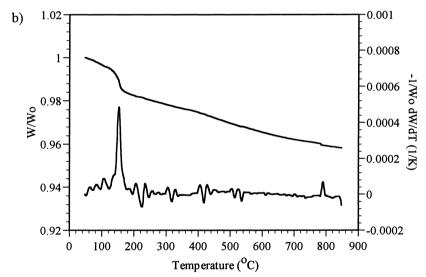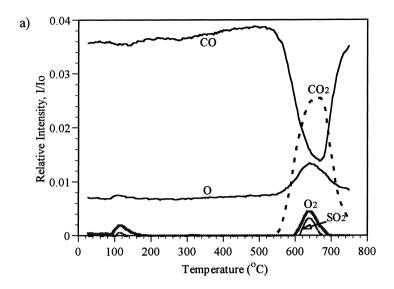
Fig. 3. H_2-TPR profiles of as prepared Cu-modified doped CeO_2 catalysts (a) 5%Cu–Ce(4.5%La)O_x, (b) 5%Cu–Ce(50%Zr)O_x, (5%H_2/He, 500 cm^3/min (STP), 10°C/min, in TGA).

isolated ions, clusters and bulk CuO particles. Cu^{+1} species were observed by XPS on the Cu-Ce(La)O_x catalysts and are considered the result of the interaction of copper oxide clusters and ceria. Under stoichiometric SO_2/CO reaction conditions, the working catalyst surface was partially sulfated [15,16].

In this work, we conducted CO-TPR experiments of pre-sulfated (400°C, 30 min in 1% SO_2/He) ceria samples. As shown in Fig. 4, reduction of sulfated

Ce(4.5%La)O_x starts at about 550°C, and is accompanied by carbon dioxide evolution. The signal corresponding to mass to charge ratio of 16 is assigned to O which may be attributed to the fragmentation of CO and CO_2 in the MS chamber. The increase in the intensity of O signal began at the same time as CO_2 evolution at 550°C due to the reduction of sulfated catalyst. In the presence of copper, the onset of reduction is shifted to lower temperature by about

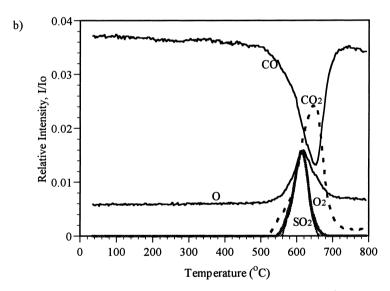Fig. 4. CO-TPR of pre-sulfated (a) Ce(4.5%La)O$_x$ and (b) 5%Cu–Ce(4.5%La)O$_x$ (2%CO/He, 50 cm^3/min (STP), 10°C/min; reactor/MS).

50°C. When the sulfate is reduced, CO can adsorb on a partially reduced ceria [57,58]. Under reaction conditions, both CO and SO$_2$ strongly adsorb on surface oxygen of ceria. The reaction can proceed at lower temperature only when a partially reduced surface is formed by the reduction of surface oxygen by CO. In the presence of copper, the lower temperature of 500°C for the onset of reduction indicates that reduction of copper/cerium sulfate precedes that of cerium

sulfate alone. Cerium and copper oxide play different roles in the redox mechanism. Cerium oxide provides the oxygen/oxygen vacancy source and disperses copper, while copper oxide increases the reducibility of ceria and provides surface sites for CO adsorption. Cu^{+1} species are stabilized by the interaction of copper oxide and ceria [15,53,54]. It is known that Cu^{+1} sites are strong sites for CO chemisorption. Although the catalyst surface becomes complex under
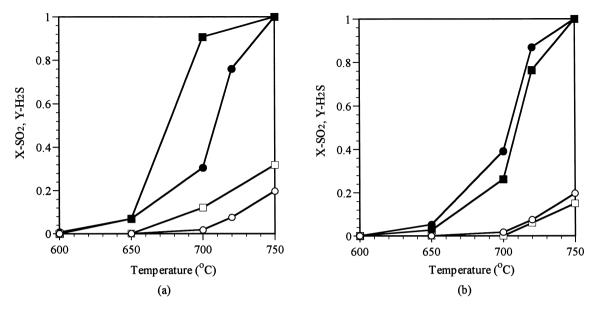
Fig. 5. SO_2 conversion and [H_2S]-yield curves in the SO_2 reduction by CH_4 over CeO_2 and $Ce(4.5\%La)O_x$ catalysts (1%SO_2–0.5%CH_4–He, 0.36 g s/cm^3) (a) 650°C-calcined, (b) 750°C-calcined, (■ □) CeO_2, (● ○) $Ce(4.5\%La)O_x$, filled symbols: X-SO_2, open symbols: Y-[H_2S].

reaction conditions [15,16], a recent study [59] indicates that Cu^{+1} provides sites for CO adsorption even in the presence of sulfur compounds.

3.2. SO_2 reduction by CH_4

As shown in Fig. 5, CeO_2 and $Ce(4.5\%La)O_x$ are active catalysts for the SO_2 reduction by CH_4. The reaction light-off temperature was about 600°C with a stoichiometric feed gas composition. Over the 650°C-calcined ceria (Fig. 5(a)), 90% SO_2 conversion and 80% sulfur yield (Y–[S]=X–SO_2–Y–H_2S) were observed at 700°C at a contact time of 0.36 g s/cm^3 (STP) (SV~20 000 h^{-1}). Catalysts with a high content of La dopant (>10 at%), which is known to produce La-enrichment of the ceria surface [53,54], were found to be less active than ceria. However, $Ce(La)O_x$ catalysts containing a small amount of La dopant (4.5–10 at%) were found to have better resistance to sintering in air and the reaction atmosphere than undoped ceria, due to a lower rate of crystallite size growth [60], as shown in Table 1. After calcination at 750°C, the La-doped catalyst showed slightly higher activity than ceria in SO_2/CH_4 tests (Fig. 5(b)). Again, the presence of excess La (20 at%) in ceria resulted in inferior performance. In many other tests, we found

that there was no significant difference between a La dopant level of 4.5 and 10 at%. Most of the catalysts reported here were doped with 4.5 at% La.

The effect of adding a small amount of copper into the $Ce(La)O_x$ catalysts was studied. The addition of 5 at% Cu had a negligible effect on the activity of $Ce(4.5\%La)O_x$ under stoichiometric conditions, as shown in Fig. 6. However, Cu modified Ce-$(4.5\%La)O_x$ showed higher selectivity to elemental sulfur under fuel-rich conditions. For example, complete conversion of SO_2 and 83% sulfur yield could be obtained at 675°C over the 5%Cu−$Ce(4.5\%La)O_x$ catalyst (720°C – calcined) at a ratio of CH_4/SO_2=2 (Fig. 6), which is four times the stoichiometric ratio for reaction 2. The light-off temperature could not be lowered below 550°C even after increasing the ratio of CH_4/SO_2 to 3. Undesirable CO as well as H_2S byproducts were detected in the product gas when the feed ratio of CH_4 to SO_2 was higher than 1 and the reaction temperature was above 650°C.

The formation of H_2S and CO at high temperature and in fuel-rich conditions suggests that partial oxidation of methane may take place over these catalysts to produce CO and H_2. Fig. 7(a) shows the difference between the CH_4 consumed and the CO_2 measured in the exit gas as a function of temperature for the
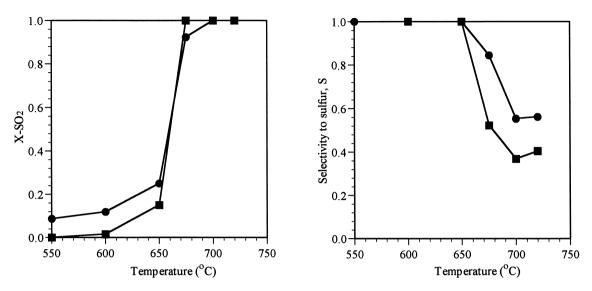
Fig. 6. Effect of catalyst composition on the light-off and sulfur selectivity of the SO_2 reduction by CH_4 over ceria-based catalysts (720°C-calcined) (1%SO_2–2%CH_4–He, 0.18 g s/cm^3), (■) Ce(4.5%La)O$_x$, (●) 5%Cu–Ce(4.5%La)O$_x$.
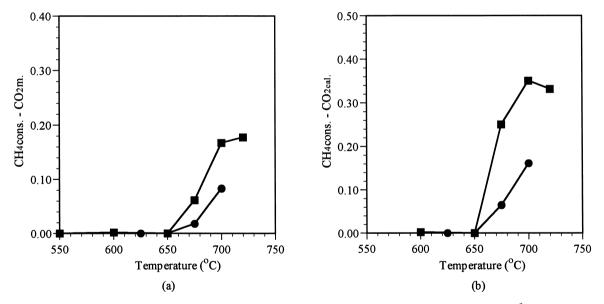

Fig. 7. Effect of catalyst composition on methane consumption and CO_2 production in 1%SO_2–2%CH_4–He, 0.18 g s/cm^3; CH_{4cons}: methane consumed, CO_{2m}: measured CO_2 production, CO_{2cal}: calculated CO_2 production on the basis of reaction 2, (■) Ce(4.5%La)O$_x$, (●) 5%Cu–Ce(4.5%La)O$_x$.

Ce(4.5%La)O$_x$ and Cu-modified catalysts. In a similar plot, Fig. 7(b) shows the difference between the CH_4 consumed and the concentration of CO_2 calculated based on the stoichiometry of reaction 2. Under fuel-rich conditions (R>0.5), the measured CO_2 product could only account for part of the CH_4 consumption, as shown in Fig. 7(a), while CO was also detected in the product gases. The amount of CO produced was equal to the difference between the measured CH_4 consumption and CO_2 production, shown in Fig. 7(a).

Apparently, methane was also consumed by partial oxidation to CO and H_2, as confirmed later by TPR experiments. This can explain the low sulfur yield at high temperature, since the H_2 produced would further react with surface sulfur to form H_2S. The difference shown in Fig. 7(b) can be referred to as the calculated CO production. This is higher than the measured CO production (Fig. 7(a)) at temperatures higher than 650°C. Therefore, the CO produced from the partial oxidation of methane may also react with SO_2 to produce CO_2 in the reaction. Copper-modified catalysts were found to suppress the excess methane consumption and CO production, as shown in Fig. 7. Therefore, the incorporation of Cu may suppress the partial oxidation of methane at high temperature and, thus, increase the catalyst selectivity to elemental sulfur. To further examine the above hypothesis, the ceria-based catalysts were tested in methane oxidation with a CH_4/O_2 molar feed ratio of 2. Partial oxidation products, CO and H_2, were observed on the $Ce(4.5\%La)O_x$ catalyst at temperatures higher than 650°C under these fuel-rich conditions. Addition of Cu into $Ce(4.5\%La)O_x$ suppressed the partial oxidation of methane up to 750°C [61].

The above results suggest the following two parallel reactions for the SO_2–CH_4 system:

$$CH_4 + 2SO_2 = 2[S] + CO_2 + 2H_2O \quad (2)$$

$$CH_4 + SO_2 = H_2S + CO + H_2O \quad (3)$$

As recognized by Nekrich et al. [21], reaction 2 represents a process with the maximum single-stage yield of sulfur and minimum acceptable level of SO_2 conversion, while reaction 3 may increase the overall conversion of SO_2, but leads to enrichment of the final mixture with H_2S and CO or H_2 at the expense of elemental sulfur. Alternatively, we may view reaction 2 as the complete oxidation of methane by SO_2, while in reaction 3, formation of partial oxidation products occurs. From the results of the present work, it appears that the addition of Cu into $Ce(La)O_x$ catalyzes reaction 2 rather than reaction 3, thus, improving the sulfur yield.

At temperatures lower than ∼550°C, the catalyst surface may be capped by SO_2. Uptake of SO_2 by $Ce(4.5\%La)O_x$ was studied in the TGA over the temperature range of 170–650°C. At each temperature, the catalyst was exposed to the 1% SO_2/He gas
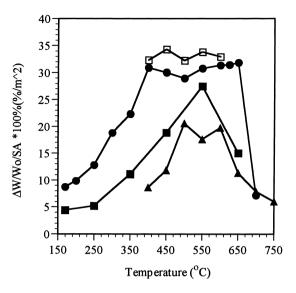

Fig. 8. Variation of SO_2 uptake with temperature over 720°C-calcined catalysts (30 min SO_2 uptake, 1% SO_2/He, 600 cm³/min), (▲) CeO_2, (■) $Ce(4.5\%La)O_x$, (●) 5%Cu–$Ce(4.5\%La)O_x$, (□) 5%Cu–$Ce(4.5\%La)O_x$ (90 min uptake).
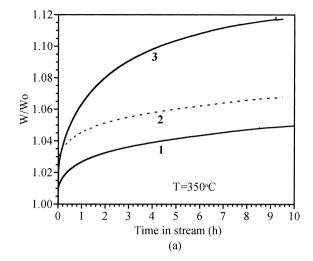
mixture for 30 min. The uptake of SO_2 increased with temperature up to 550°C, as indicated in Fig. 8. A steep decrease was observed from 550°C to 650°C, which is attributed to reduced thermal stability of the sulfate species. Recent IR studies of CeO_2 sulfation [62] have shown that surface sulfate of cerium as well as bulk cerium sulfate can be formed upon exposure to SO_2 even without O_2 in the gas phase. A large increase in the formation of bulk sulfate was observed above 500°C [62]. However, the thermal stability of bulk sulfate in He was found to be lower than that of the surface sulfate. In our experiments we observed no weight loss in He by removing the SO_2 from the feed gas, if the temperature was lower than 550°C. Apparently, stable sulfate species were present up to this temperature. At higher temperature, reversible and irreversible adsorption of SO_2 was observed. According to the IR studies of Waqif et al. [62], a large part of the bulk cerium sulfate had decomposed after evacuation at 600°C. In addition, Liu et al. [16] have reported that at a temperature around 550°C, the desorption of SO_2 from copper modified ceria became significant in the absence of gaseous SO_2. Thus, bulk sulfate, which is formed above a certain temperature, will decompose in He due to its low thermal stability. Surface sulfate species may decompose at higher temperature.

Although it is difficult to differentiate between the decomposition of bulk and surface sulfate in our experiments, the data suggest that a decrease in the overall SO_2 adsorption capacity may be caused by the lower thermal stability of sulfates at high temperature.

The addition of 5 at% Cu changed the SO_2 adsorption behavior significantly. Fig. 8 shows that the SO_2 uptake for the $5\%Cu–Ce(4.5\%La)O_x$ was higher than that of $Ce(4.5\%La)O_x$. The weight increase due to sulfation of the copper oxide in this material should not exceed 1.86 wt% (corresponding to 5–7.5 wt%/ m^2, depending on the amount of catalyst used in the uptake experiments), which was calculated by assuming that all the copper in the catalyst existed as fully exposed cupric oxide, which was all sulfated (1:1, SO_2:CuO). This value is smaller than the corresponding difference measured between the $Ce(4.5\%La)O_x$ and $5\%Cu–Ce(4.5\%La)O_x$ samples in the 30 min SO_2 uptake experiments at $T>250°C$ (Fig. 8), except at 550°C, indicating that copper increases the uptake of SO_2 by $Ce(4.5\%La)O_x$.

A plateau is observed for the Cu-containing sample at 400–675°C after 30 min SO_2 uptake. The exposure time of SO_2 uptake on $5\%Cu–Ce(4.5\%La)O_x$ was extended to further check this issue. A similar profile was obtained in the temperature range of 400–600°C after 90 min exposure to the $1\%SO_2$/He mixture, with a slightly higher weight increase than that obtained in 30 min SO_2 uptake, as shown in Fig. 8. These results suggest the formation of sulfate species of different thermal stability. It has been reported by Twu et al. [63] that bulk-like sulfate species $Ce_2(SO_4)_3$, generated at temperatures higher than 400°C, is thermally stable up to 650°C at ambient conditions. The addition of copper complicates the picture because of the different stability of its own bulk and surface sulfates. However, the enhancement of sulfation of ceria induced by copper is clear in Fig. 8.

Two SO_2 uptake isotherms are shown in Fig. 9. At the temperature of 350°C, the excess SO_2 uptake due to the addition of copper continues to increase with the exposure time up to 9 h, exhibiting a large enhancement of the uptake of SO_2 by $Ce(La)O_x$ at this temperature. This may be correlated to the enhanced oxygen storage of ceria induced by the presence of copper (Table 2). A smaller effect is observed at the temperature of 450°C, as shown in Fig. 9(b). As bulk sulfates of ceria begin to form at temperatures higher
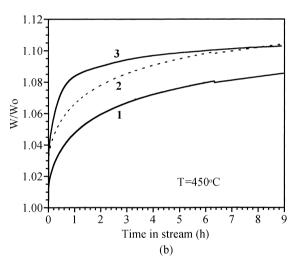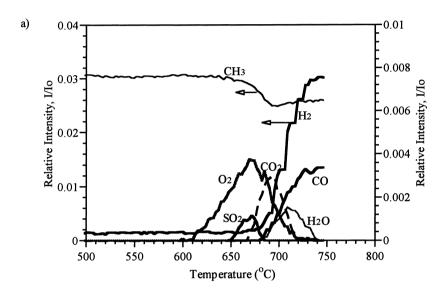

Fig. 9. SO_2 uptake isotherms over $Ce(4.5\%La)O_x$ and $5\%Cu–Ce(4.5\%La)O_x$ at (a) 350°C, (b) 450°C in $1\%SO_2$/He (600 cm^3/ min); (1) measured SO_2 uptake on $Ce(4.5\%La)O_x$, (2) calculated value of W/W_0 on the basis of 1 and the stoichiometric uptake of SO_2 by copper present in the $5\%Cu–Ce(4.5\%La)O_x$ sample, (3): measured SO_2 uptake on $5\%Cu–Ce(4.5\%La)O_x$.

than 400°C [62,63], their amount increasing with time, the addition of copper does not contribute much to the overall SO_2 uptake. However, it still enhances the uptake of SO_2 by $Ce(La)O_x$ at short exposure times due to a higher rate of sulfation, as shown in Fig. 9(b). Benedek and Flytzani-Stephanopoulos [64] have reported an enhancement of the sulfation of ceria by the addition of copper in simulated flue gas streams (containing both SO_2 and O_2). The enhanced uptake of

SO_2 is attributed to the higher oxygen supply induced by copper, since surface oxygen species are active sites for SO_2 adsorption.

The SO_2 uptake experiments have indicated that sulfate species start to decompose at a temperature of ∼550°C, which coincides with the light-off temperature of the $CH_4 + SO_2$ reaction. Confirmation of this was obtained by CH_4-TPR of pre-sulfated catalysts as shown in Fig. 10. Oxygen started to desorb at 600°C

before the elution of SO_2 in TPR experiments. This oxygen desorption was not observed in the CH_4-TPR experiments of fresh catalysts. Therefore, it is attributed to the decomposition of a sulfate species. The decrease of the methyl signal (15 amu) began at the same time as the O_2 elution at 600°C. This temperature was almost the same as the corresponding temperature of the onset of thermal decomposition of sulfate species in He. Moreover, similar results were
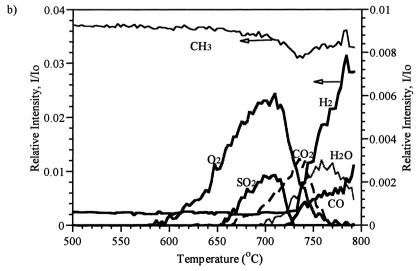

Fig. 10. CH_4-TPR profiles (reactor/MS) of pre-sulfated catalysts in 2%CH_4/He, (a) Ce(4.5%La)O_x, (b) 5%Cu–Ce(4.5%La)O_x; catalysts pre-sulfated with 1% SO_2/He at 400°C for 30 min (10°C/min, 150 mg, 50 cm^3/min).

obtained in CH$_4$-TPR and He-TPD experiments of the pre-sulfated Ce(4.5%La)O$_x$ material carried out in the TGA, i.e., the catalyst weight started to decrease at the same temperature. Therefore, we conclude that methane activation over the sulfated catalysts can occur only after partial decomposition of the sulfated surface. Partial oxidation products, H$_2$ and CO, were also detected on the partially sulfated Ce(4.5%La)O$_x$ catalyst at ~680°C (Fig. 10(a)), at which temperature a significant amount of H$_2$S was formed under reaction conditions (Fig. 6). Methane may react with the lattice oxygen at high temperature producing partial oxidation products.

The CH$_4$-TPR profiles of the pre-sulfated catalysts showed different behavior for the copper-modified ceria materials, as shown in Fig. 10(b). The evolution of H$_2$ and CO over 5%Cu–Ce(4.5%La)O$_x$ was shifted to higher temperature. CuO provides active sites for the complete oxidation of methane [15,55,65]. The present results support the assumption that copper suppresses the partial oxidation of methane during the reaction of SO$_2$+CH$_4$, which may then be the reason for the higher selectivity to elemental sulfur obtained with this catalyst (reaction 2). No methane activation was observed at temperature lower than 550°C over the pre-sulfated catalysts. Deberry and Sladek [66] reported that CuO can form bulk sulfates in the presence of SO$_2$ and O$_2$ at 325°C. Although there is no O$_2$ present in the reaction mixture of CH$_4$+SO$_2$, stable surface sulfates of CuO may still be formed, due to adsorption of SO$_2$ on copper oxide. Previous XPS studies of Cu–Ce(4.5%La)O$_x$ catalysts by Liu and coworkers [15,16] have shown that the working catalyst comprises copper oxide, sulfide and sulfate as well as cerium oxide and sulfate in the CO+SO$_2$ reacting atmosphere. Therefore, at low temperature, metal oxides may form surface sulfates during the reaction which do not provide sites for methane activation. The activity of the metal-modified ceria catalysts then depends on the thermal stability of the metal sulfate. This is further supported by the results shown in Fig. 11. This figure shows plots of (1-conversion) versus time for the pre-sulfated 5%Cu–Ce(4.5%La)O$_x$ sample heated in various gases at 550°C. The same initial slope for the thermal decomposition profile in He and the reduction profile in CH$_4$ was measured for this material. A faster initial reduction is shown in the CO/He gas mixture.
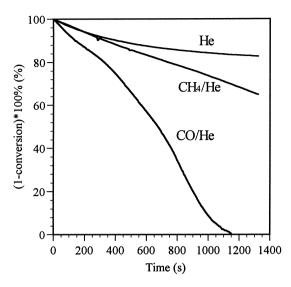

Fig. 11. Isothermal reduction/decomposition profiles of pre-sulfated (400°C, 30 min in 1% SO$_2$/He) 5%Cu–Ce(4.5%La)O$_x$ at 550°C. Reduction with 5%CH$_4$/He or 2%CO/He (600 cm^3/min), decomposition in He (600 cm^3/min), all in the TGA.

Due to the formation of sulfate species over the ceria-based catalysts in the presence of SO$_2$, methane activation cannot take place until the sulfate begins to decompose thermally. Thus, the activity of the ceria-based catalysts for the SO$_2$+CH$_4$ reaction is limited by sulfate decomposition. However, as shown in Fig. 11, the reduction of pre-sulfated 5%Cu–Ce(4.5%La)O$_x$ with CO is a much faster process than that with CH$_4$ showing a higher slope throughout the reduction period. In fact, the reaction of CO+SO$_2$ can proceed at temperatures lower than 550°C when a partially sulfated surface is available by pre-reduction with CO (Fig. 2). A similar pre-reduction of the ceria did not help to initiate the CH$_4$+SO$_2$ reaction at temperatures below 550°C [61].

4. Conclusion

La-doped ceria is a highly active catalyst for SO$_2$ reduction by CO and CH$_4$. In the case of reduction by CO, formation of surface defects (oxygen vacancies) and ceria reducibility are important for catalyst activity. The reaction can be explained by the redox mechanism. SO$_2$ adsorbs strongly on the catalyst surface forming sulfates. Partial reduction of sulfate

by CO is necessary for the reaction to proceed at low temperature. The reaction thus takes place over surface oxygen vacancy sites, which are created by reduction by CO. The reaction is facilitated by CO adsorption on partially reduced ceria. Addition of copper improves the low temperature reducibility of ceria, and consequently the activity. Moreover, strong interaction between copper and ceria stabilizes Cu^{+1} species, which provide additional sites for CO adsorption.

Using methane as the reductant is different from CO, since methane activation requires surface oxygen species. Strong adsorption of SO_2 on all the CeO_2-based catalysts examined in this work inhibits methane activation at temperatures below $550°C$. The reaction between SO_2 and CH_4 begins on a partially sulfated catalyst. Thus, the light-off temperature of ceria-based catalysts depends on the thermal stability of the sulfates. The activation of methane may involve surface oxygen species [55,67,68] and partially reduced metal oxide sites at high temperature. Two independent reactions are proposed and used to explain the catalytic performance of ceria-based oxides. The addition of copper increases the selectivity to elemental sulfur under fuel-rich conditions by catalyzing the complete oxidation of methane.

Acknowledgements

References

[1] Steam Electric Plant Factors, 1992 ed., National Coal Association.

[2] D.S. Henzel, W. Ellison, Commercial utilization of SO_2 removal wastes in the application of new advanced control technology, Proceeding of the 1990 SO_2 Control Symposium, vol. 1, p. 3B-27.

[3] S. Tyson, Guidance for coal ash use: codes and standards activities for high volume applications, Proceedings of the Ninth Annual International Pittsburgh Coal Conference, October 1992.

[4] J.M. Whelan, US Patent 4 081 519 (1978).

[5] J. Happel, M.A. Hnatow, L. Bajars, M. Kundrath, Ind. Eng. Chem. Prod. Res. Dev. 14(3) (1975) 154.

[6] J. Happel, A.L. Leon, M.A. Hnatow, L. Bajars, Ind. Eng. Chem. Prod. Res. Dev. 16(2) (1977) 150.

[7] D.B. Hibbert, R.H. Campbell, Appl. Catal. 41 (1988) 273.

[8] D.B. Hibbert, R.H. Campbell, Appl. Catal. 41 (1988) 289.

[9] N.Q. Minh, J. Am. Ceram. Soc. 76(3) (1993) 563.

[10] J.A. Baglio, Ind. Eng. Chem. Prod. Res. Dev. 21 (1982) 38.

[11] Y. Jin, Q. Yu, S.G. Chang, US Patent 5 494 879 (1996).

[12] S.D. Gangwal, W.J. McMicheal, T. Dorchak, Environ. Progr. 10(3) (1991) 186.

[13] W. Liu, A.F. Sarofim, M. Flytzani-Stephanopoulos, Appl. Catal. B 4 (1994) 167.

[14] M. Flytzani-Stephanopoulos, W. Liu, US Patent no. 5 384 301 (1995).

[15] W. Liu, Sc.D. Thesis, Massachusetts Institute of Technology, May 1995.

[16] W. Liu, C. Wadia, M. Flytzani-Stephanopoulos, Catal. Today 28 (1996) 391.

[17] J.J. Helstrom, G.A. Atwood, Ind. Eng. Chem. Process Des. Dev. 17 (1978) 114.

[18] J. Sarlis, D. Berk, Ind. Eng. Chem. Res. 27 (1988) 1951.

[19] D.J. Mulligan, D. Berk, Ind. Eng. Chem. Res. 28 (1989) 926.

[20] T.S. Wiltowski, K. Sangster, W.S. O'Brien, J. Chem. Tech. Biotech. 7 (1996) 204.

[21] E.M. Nekrich, A.N. Kontsevaya, G.F. Ganzha, J. Appl. Chem. U.S.S.R. 51 (1978) 517.

[22] D.J. Mulligan, D. Berk, Ind. Eng. Chem. Res. 31 (1992) 119.

[23] J. Sarlis, D. Berk, Chem. Eng. Commun. 140 (1996) 73.

[24] J.J. Yu, Q. Yu, Y. Jin, S.G. Chang, Ind. Eng. Chem. Res. 36 (1997) 2128.

[25] V.A. Zazhigalov, S.V. Gerei, M. Rubanik, Kinet. Katal. 4 (1975) 967.

[26] T. Chivers, J.B. Hyne, C. Lau, Int. J. Hydrogen Energy 5 (1980) 499.

[27] S.C. Moffat, A.A. Adesina, Catal. Lett. 37 (1996) 167.

[28] M.M. Akhmedov, G.B. Shakhtakhtinskii, A.I. Agaev, S.S. Gezalov, Zhurnal Prikladnoi Khimii 59 (1986) 504.

[29] A. Tschope, W. Liu, M. Flytzani-Stephanopoulos, J.Y. Ying, J. Catal. 157 (1995) 42.

[30] A. Trovarelli, Catal. Rev.-Sci. Eng. 38(4) (1996) 439.

[31] H.L. Tuller, A.S. Nowick, J. Electrochem. Soc. 2 (1975) 255.

[32] H. Inaba, H. Tagawa, Solid State Ionics 83 (1996) 1.

[33] C. De Leitenburg, A. Trovarelli, J. Llorca, F. Cavani, G. Bini, Appl. Catal. A 131 (1995) 161.

[34] P. Fornasiero, R. Di Monte, G. Ranga Rao, J. Kaspar, S. Meriani, A. Trovarelli, M. Graziani, J. Catal. 151 (1995) 168.

[35] F. Zamar, A. Trovarelli, C. De Leitenburg, G.J. Dolcetti, Chem. Soc. Chem. Commun. 9 (1995) 965.

[36] G. Balducci, P. Fornasiero, R. Di Monte, J. Kaspar, S. Meriani, M. Graziani, Catal. Lett. 33 (1995) 193.

[37] Y. Amenomiya, A. Emesh, K. Oliver, G. Pleizer, in: M. Philips, M. Ternan (Eds.), Proceedings of the Ninth International Congress on Catalysis, Chemical Institute of Canada, Ottawa, 1988, p.634.

[38] P. Malet, A. Caballero, J. Chem. Soc., Faraday Trans. 1 84(7) (1988) 2369.

[39] Y.-M. Chiang, E.B. Lavic, I. Kosacki, H.L. Tuller, J.Y. Ying, Appl. Phys. Lett. 69(2) (1996) 8.

[40] M.H. Yao, R.J. Baird, F.W. Kunz, T.E. Hoost, J. Catal. 166 (1997) 67.

[41] B. Harrison, A.F. Diwell, C. Hallet, Platinum Metals Rev. 32(2) (1988) 73.

[42] G.S. Zafiris, R.J. Gorte, J. Catal. 139 (1993) 561.

[43] H. Cordatos, R.J. Gorte, J. Catal. 159 (1996) 112.

[44] H. Cordatos, T. Bunluesin, J. Stubenrauch, J.M. Vohs, R.J. Gorte, J. Phys. Chem. 100 (1996) 785.

[45] E.S. Putna, J.M. Vohs, R.J. Gorte, J. Phys. Chem. 100 (1996) 17862.

[46] T. Bunluesin, R.J. Gorte, G.W. Graham, Appl. Catal. B 339 (1997) 1.

[47] A.L. Tarasov, L.K. Przheval'skaya, V.A. Shvets, V.B. Kazanskii, Kinet. Katal. 29(5) (1988) 1181.

[48] C. Li, Y. Chen, W. Li, Q. Xin, in: T. Inui et al. (Eds.), New Aspects of Spillover in Catalysis, Elsevier, Amsterdam, 1993, p. 217.

[49] H.C. Yao, Y.F.Y. Yao, J. Catal. 86 (1984) 254.

[50] J.G. Nunan, R.G. Silver, S.A. Bradley, in: R.G. Silver, J.E. Saeyer, J.C. Summers (Eds.), Catalytic Control of Air Pollution, Chapter 17, ACS Symposium Series, vol. 495, American Chemical Society, Washington, DC, 1992.

[51] A. Aboukais, A. Bennani, C.F. Aissi, M. Guelton, J.C. Vedrine, Chem. Mater. 4 (1992) 977.

[52] J. Soria, J.C. Conesa, A. Martinez-Arias, J.M. Coronado, Solid State Ionics, 63–65 (1993) 755.

[53] W. Liu, M. Flytzani-Stephanopoulos, J. Catal. 153 (1995) 304.

[54] W. Liu, M. Flytzani-Stephanopoulos, J. Catal. 153 (1995) 317.

[55] L. Kundakovic, M. Flytzani-Stephanopoulos, Appl. Catal. A 171 (1998) 13.

[56] W. Liu, M. Flytzani-Stephanopoulos, Chem. Eng. J. 64 (1996) 283.

[57] C. Li, Y. Sakata, T. Arai, K. Domen, K. Maruya, T. Onishi, J. Chem. Soc., Faraday Trans. 1 85(4) (1989) 929.

[58] C. Li, Y. Sakata, T. Arai, K. Domen, K. Maruya, T. Onishi, J. Chem. Soc., Faraday Trans. 1 85(6) (1989) 1451.

[59] M.B. Badley, C.H. Rochester, G.J. Hutchings, F.J. King, J. Catal. 148 (1994) 438.

[60] M. Pijolat, M. Print, M. Soustelle, Solid State Ionics, 63–65 (1993) 781.

[61] T. Zhu, Ph.D. Thesis, Tufts University, in preparation.

[62] M. Waqif, P. Bazin, O. Sanr, J.C. Lavalley, G. Blanchard, O. Touret, Appl. Catal. B 11 (1997) 193.

[63] J. Twu, C.J. Chuang, K.I. Chang, C.H. Yang, K.H. Chen, Appl. Catal. B 12 (1997) 309.

[64] K. Benedek, M. Flytzani-Stephanopoulos, Cross-Flow, Filter–Sorbent–Catalyst for Particulate, SO_2 and NO_x Control, Final report to the US Dept. of Energy, A.D. Little, Inc., Contract no. 22-89PC89805, May 1994.

[65] G. Wrobel, C. Lamonier, A. Bennani, A. D'Huysser, A. Aboukais, J. Chem. Soc., Faraday Trans. 92 (1996) 2001.

[66] D.W. Deberry, K.J. Sladek, Canadian J. Chem. Eng. 49 (1971) 781.

[67] C. Li, Q. Xin, J. Phys. Chem. 96 (1992) 7714.

[68] R.O. Long, Y.P. Huang, H.L. Wan, J. Raman Spectrosc. 28 (1997) 29.